Vascular Inflammation Imaging with ^{18}F-FDG PET/CT: When to Image?

Leon J. Menezes[1], Carl W. Kotze[2], Brian F. Hutton[1], Raymondo Endozo[1], John C. Dickson[1], Ian Cullum[1], Syed W. Yusuf[2], Peter J. Ell[1], and Ashley M. Groves[1]

[1]Institute of Nuclear Medicine, University College Hospital, University College London, London, United Kingdom; and [2]Brighton and Sussex University Hospital, Brighton, Sussex, United Kingdom

We prospectively investigated the ideal imaging time to measure vascular uptake after injection of ^{18}F-FDG. **Methods:** A total of 17 patients with atherosclerotic abdominal aortic aneurysm underwent dynamic abdominal PET/CT using 2-min frames between 45 and 53, 57 and 65, 115 and 123, and 175 and 183 min after injection of ^{18}F-FDG. For each period of dynamic imaging, vessel wall and lumen uptake were measured using the maximum standardized uptake value (SUV$_{max}$) and target-to-background ratio (TBR). **Results:** No significant difference in TBR across all time points (repeated measures ANOVA, $P = 0.206$) was observed, despite a significant difference in aortic wall and lumen uptake with time (repeated measures ANOVA, $P = 0.02$ and $P < 0.001$, respectively). There was no significant difference between aortic wall uptake at 60 min (SUV$_{max}$, 2.15 ± 0.11 SE) and 180 min (SUV$_{max}$, 1.99 ± 0.18 SE) (paired t test, $P = 0.367$). There was a significant difference in lumen uptake at 60 min (SUV$_{max}$, 2.4 ± 0.11 SE) and 180 min (SUV$_{max}$, 1.7 ± 0.1 SE) (paired t test, $P = 0.001$). There was no significant difference in TBR between 60 min (0.91 ± 0.03) and 180 min (1.01 ± 0.06 SE) (paired t test, $P = 0.131$). With increasing delayed imaging, there was increasing variability (SE) in the SUV$_{max}$ for the aortic wall and TBRs. **Conclusion:** There was no significant advantage in imaging at 3 h over 1 h after ^{18}F-FDG injection.

Key Words: PET/CT; vascular; radiotracer tissue kinetics; ^{18}F-FDG; aneurysm; atherosclerosis; methodology; positron emission tomography

PET with ^{18}F-FDG has shown potential in the imaging of atheroma inflammation and instability in both the carotid artery and aorta (1–4). This original work has progressed, and ^{18}F-FDG PET is being suggested for use in measuring the response to cardiovascular treatment and as a surrogate endpoint in clinical trials (5–9). However, a paucity of scientific evidence regarding the technical parameters of using PET in this way exists.

One important parameter is the circulation time of ^{18}F-FDG. The 1-h time point is commonly used in oncology PET studies (10). However, some have advocated performing imaging at 3 h after the injection of ^{18}F-FDG to maximize the contrast between plaque and background. The 3-h time point was derived from dynamic PET studies in patients with carotid disease (1). However, this time point was based on data from a PET-only system in which physical coregistration with CT was not possible, and data were from only 8 patients. Not all investigators have used this time point (Table 1), and more recently these same investigators have recommended at least a 90-min ^{18}F-FDG circulation time (8). Therefore, there is a need for harmonization of scan parameters to enable comparison and collaboration between institutions offering vascular PET/CT.

To address this question of the ideal circulation time of ^{18}F-FDG, we scanned patients with atherosclerotic abdominal aortic aneurysms. We performed PET/CT at 45, 60, 120, and 180 min after an injection of ^{18}F-FDG. We investigated whether there were ^{18}F-FDG uptake differences with time in the aortic wall and lumen of the aneurysms to determine the optimal time to image vascular inflammation using ^{18}F-FDG PET/CT.

MATERIALS AND METHODS

Study Population

A total of 17 consecutive asymptomatic patients (16 men, 1 woman; mean age, 74 ± 5 y) undergoing routine surveillance for atherosclerotic abdominal aortic aneurysms enrolled in this prospective study. The clinical and laboratory characteristics of the study population are presented in Table 2. A total of 9 patients had hypercholesterolemia, 10 were receiving statins, and 9 had a smoking history. No patients had any renal impairment or any features of an inflammatory aneurysm (11). Institutional Ethics Board approval and informed consent were obtained.

Image Acquisition

All patients fasted for 6 h. After an injection of ^{18}F-FDG (200 MBq), we performed dynamic imaging using 2-min frames between 45 and 53, 57 and 65, 115 and 123, and 175 and 183 min with a combined PET/64-detector CT instrument (GE Healthcare). A CT scan of the patient's abdominal aorta was acquired using 64 × 3.75 mm detectors, a 1.5 pitch, and a 5-mm collimation

TABLE 1. Published Prospective Human Studies of ^{18}F-FDG PET Atherosclerosis Imaging

Reference	No. of patients	Circulation time (min)	PET scan type	Method of image analysis
Sakalihasan et al. (14)	26	60	PET only	Visual
Rudd et al. (1)	8	180	PET only	Net ^{18}F-FDG accumulation rate
Davies et al. (15)	12	120	PET only	Uptake ratio > 1.28
Tawakol et al. (2)	17	180	PET only	TBR
Okane et al. (16)	15	103–158	PET only	TBR
Tahara et al. (7)	43	60	PET only	SUV_{max}
Wu et al. (12)	47	45 and 150	PET/CT	SUV_{max} > 2.0
Lee et al. (9)	60	45	PET/CT	Uptake ratio > 1
Arauz et al. (17)	13	90	PET only	Visual, $SUV_{max} \geq 2.7$
Rudd et al. (5)	11	90	PET/CT	TBR
Tahara et al. (18)	216	60	PET only	SUV score
Tahara et al. (13)	100	60	PET only	SUV score ≥ 1.60
Kuehl et al. (19)	33	60	PET/CT	SUV_{max} > 2.5
Paulmier et al. (20)	45	60	PET/CT	SUV_{max}
Rudd et al. (8)	20	90	PET/CT	TBR
Reeps et al. (4)	15	90	PET/CT	SUV_{max}

(140 kVp and 80 mA in 0.8 s). An ^{18}F-FDG PET emission scan was obtained while the patient's position was maintained; the scan covered an area identical to that covered by CT. All scans were acquired in 2-dimensional mode (8 min/bed position). Transaxial emission images, 3.27 mm thick (pixel size, 3.9 mm), were reconstructed using ordered-subsets expectation maximization with 2 iterations and 28 subsets. The axial field of view was 148.75 mm, resulting in 47 slices per bed position.

Image Analysis

Coregistration and image analysis were performed using a Xeleris (GE Healthcare) workstation. PET/CT images were reviewed by a combined radiologist and nuclear medicine physician and a senior technologist in consensus. The area of most intense aortic wall ^{18}F-FDG uptake was identified, and regions of interest (ROIs) were drawn over the abdominal aortic wall and lumen (Fig. 1). The maximum activity concentration for each region was recorded in each 2-min frame. For each period of dynamic imaging (four 2-min frames), the mean maximum activity concentration (corrected for decay) was recorded and converted to maximum standardized uptake value (SUV_{max}) normalized to body weight, calculated using the following formula:

$$SUV = \frac{ROI \; decay - corrected \; activity \; (kBq)/tissue \; (mL),}{injected \, ^{18}F - FDG \; dose \; (kBq)/body \; weight \; (g)}$$

and the associated SE (SD/$\sqrt{4}$) was derived. This calculation was repeated in each of the 17 patients, and mean SUV_{max} for the aortic wall and lumen and their target-to-background ratio (TBR) were derived.

Statistical Analysis

After data were examined for normality using Kolmogorov–Smirnov testing, ANOVA of repeated measures was used in the comparison of uptake across all the 4 time points. A paired

TABLE 2. Clinical Characteristics of Study Population

Characteristic	n
Age (mean ± SD)	74 ± 5 y
Male	16
Female	1
Body mass index (mean ± SD)	25.7 ± 4 kg/m^2
Diabetes mellitus	2
Fasting blood glucose (mean ± SD)	5.2 ± 0.9
Hypertension	8
Hyperlipidemia	9
Current smoker	2
Ex-smoker	7
Renal impairment	0
Raised c-reactive protein	1
Raised ESR	3
Statin therapy	10
Angiotensin-converting enzyme inhibitor therapy	6
β-blocker therapy	3
Maximum AAA diameter (mean ± SD)	5.3 ± 0.9 cm

ESR = erythrocyte sedimentation rate; AAA = abdominal aortic aneurysm.
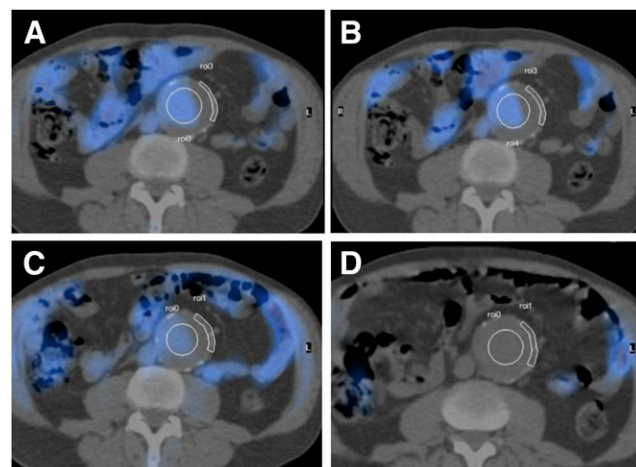

FIGURE 1. Fused axial PET/CT of ROIs applied to aortic aneurysmal wall and lumen at mid-point of dynamic acquisitions at 45 (A), 60 (B), 120 (C), and 180 min (D) after injection of ^{18}F-FDG.

2-tailed *t* test was used to compare differences between variables obtained at 1 and 3 h. Statistical significance was at 5%.

RESULTS

The mean aortic wall SUV_{max} at 45 min was 2.08, at 60 min it was 2.15, at 120 min it was 1.62, and at 180 min it was 1.99. The mean aortic lumen SUV_{max} at 45 min was 2.30, at 60 min it was 2.40, at 120 min it was 1.74, and at 180 min it was 1.70. The mean wall-to-lumen ratio (TBR) at 45 min was 0.91, at 60 min it was 0.91, at 120 min it was 0.96, and at 190 min it was 1.01 (Table 3).

The SDs and SEs for aortic wall SUV_{max} and lumen SUV_{max} and TBRs at 45, 60, 120, and 180 min after injection of ^{18}F-FDG are shown in Table 3.

A significant difference in aortic wall SUV_{max} and lumen SUV_{max} with time (repeated measures ANOVA, $P = 0.02$ and $P < 0.001$, respectively) and no significant difference in TBR with time (repeated measures ANOVA, $P = 0.206$) were observed.

At the 2 specific time points of interest, there was no significant difference between SUV_{max} at 60 and 180 min in the aortic wall (paired *t* test, $P = 0.367$). There was a significant difference in SUV_{max} in the lumen at 60 and 180 min (paired *t* test, $P = 0.001$). There was no significant difference in TBR SUV_{max} between 60 and 180 min (paired *t* test, $P = 0.131$).

DISCUSSION

We conducted a study in a series of 17 patients with abdominal aortic aneurysms, which are strongly associated with both local and systemic atherosclerosis (*11*), to determine the optimal time to image vascular inflammation using ^{18}F-FDG PET/CT. Multiple–time point PET of arterial ^{18}F-FDG uptake showed that delayed imaging at 3 h,

compared with earlier imaging, does not significantly change the TBR. There was also no difference in aortic wall SUV_{max} at 1 h, compared with at 3 h. Blood-pool activity as measured by lumen SUV_{max} was significantly different at 1 and 3 h, but this did not affect the TBR.

Given that there is increasing use of ^{18}F-FDG uptake to assess arterial inflammation and atheroma vulnerability and to monitor the effects of pharmacologic therapies (*1–9*), these findings are likely to be relevant to this emerging technique. In addition, showing that there is no significant advantage of delayed imaging could favorably impact clinical practice. The prior recommended imaging time of 3 h (*1*) that has been implemented by others (*2*) could limit the feasibility in some centers of performing future screening or drug monitoring using ^{18}F-FDG PET. By imaging at 1 h, this should allow a better workflow for imaging departments and make the ^{18}F-FDG PET examination more acceptable to the patient, which is an important factor for any test.

We have also shown that the measurement of ^{18}F-FDG arterial wall uptake becomes more variable with delayed imaging, most probably because of the resulting decay of the tracer and the subsequent increase in image noise. Therefore, the possible benefits of delayed imaging are counterbalanced by the effects of image noise and more variable SUV_{max} measurements. Given the relatively subtle changes involved in the imaging of atherosclerotic lesions with ^{18}F-FDG PET, such variability may negatively affect the findings if imaging is delayed.

Imaging at 2 h showed a decline in ^{18}F-FDG arterial wall uptake, a finding that was replicated in all but 6 of our patients. Although it is hard to explain such an uptake pattern, this finding could raise concern about the recommended use of imaging at 90 min (*8*).

Although PET has exquisite sensitivity, it does have limited spatial resolution. Therefore, using this technique to examine the arterial wall is a challenge, and it can be difficult to accurately localize the site of uptake from PET. This is one of the reasons for choosing to examine the aorta in this study, rather than the smaller carotid arteries. The addition of CT when using a hybrid PET/CT camera for image acquisition enables the exploitation of the superior spatial resolution of CT and thus improves the anatomic certainty of the site of ^{18}F-FDG uptake. In particular, the use of a hybrid system helps differentiate arterial wall uptake from uptake in adjacent structures such as the lumen, which should help in the placement of ROIs and reduction of partial-volume effects. The CT used for image fusion was unenhanced; therefore, the thrombus within the sac of the aneurysm may make identification of the lumen more difficult with unenhanced CT, compared with contrast-enhanced CT. The original arterial wall uptake data suggesting that 3 h was the best imaging time (*1*) were acquired from the carotid arteries using a standalone PET camera, and the findings of this study may have been influenced by these factors of poor spatial resolution, partial-volume effects, and inaccurate ROI localization.

TABLE 3. Data for SUV_{max} of Aortic Wall, Aortic Lumen, and TBR at Each Time Point After Injection of ^{18}F-FDG

Area	Time (min)			
Wall	45	60	120	180
Mean	2.08	2.15	1.62	1.99
% change	0	+3%	−22%	−4%
SD	0.44	0.46	0.26	0.745
SE	0.11	0.11	0.62	0.18
Lumen				
Mean	2.3	2.4*	1.74	1.7*
% change	0	+4%	−24%	−26%
SD	0.4	0.44	0.41	0.4
SE	0.1	0.11	0.1	0.1
TBR				
Mean	0.91	0.91	0.96	1.01
% change	0	0	+6%	+11%
SD	0.16	0.14	0.15	0.26
SE	0.04	0.03	0.03	0.06

*Significant difference in SUV_{max} in lumen at 60 and 180 min (paired *t* test, $P = 0.001$) was observed.

There has been an inconsistent use of methodology when performing PET vascular studies (Table 1). Different investigators have used a variety of strategies in expressing arterial ^{18}F-FDG uptake, including visual assessment, absolute SUV_{max}, SUV thresholds, and TBR. Likewise, there has been a variety of imaging times used, ranging from 45 min (9,12) to 3 h. These inconsistencies probably reflect multiple factors, including habit and the demand for camera availability (13). Therefore, as is being sought (8), there is a need for the uniformity of methodology for arterial ^{18}F-FDG studies.

One recent vascular ^{18}F-FDG PET study did obtain dual–time point imaging data (12). In this study, it was noted that the delayed images provided better lesion-to-background contrast during visual assessment. However, the pattern and location of ^{18}F-FDG uptake could be identified on both early and delayed images in all patients with significant carotid stenosis. Moreover, because the ^{18}F-FDG uptake on delayed images greatly decreased in the control subjects, making it difficult for ROI placement along the arterial wall, the 45-min images were used for SUV comparison.

In the current study, we performed dynamic imaging during certain time points; however, it would have been ideal to have obtained continuous dynamic images over 3 h. In practice, with elderly patients, continuous dynamic imaging may be difficult to achieve; moreover, the images would be at an increased risk of movement-induced artifacts. It would have been advantageous to have performed studies on more than the 17 patients studied. Nonetheless, such studies are time-intensive, and most of the present ^{18}F-FDG PET arterial studies have used similar-sized or smaller study populations (Table 1).

CONCLUSION

Our prospective aortic wall PET data from 17 patients showed that there was no significant advantage in imaging at 3 h over 1 h after ^{18}F-FDG injection. Given the increasing use of vascular ^{18}F-FDG PET studies for risk stratification and treatment monitoring, this finding has implications for patient throughput and acceptability.

ACKNOWLEDGMENTS

REFERENCES

1. Rudd JH, Warburton EA, Fryer TD, et al. Imaging atherosclerotic plaque inflammation with [^{18}F]-fluorodeoxyglucose positron emission tomography. *Circulation*. 2002;105:2708–2711.
2. Tawakol A, Migrino RQ, Bashian GG, et al. In vivo ^{18}F-fluorodeoxyglucose positron emission tomography imaging provides a noninvasive measure of carotid plaque inflammation in patients. *J Am Coll Cardiol*. 2006;48:1818–1824.
3. Tatsumi M, Cohade C, Nakamoto Y, Wahl RL. Fluorodeoxyglucose uptake in the aortic wall at PET/CT: possible finding for active atherosclerosis. *Radiology*. 2003;229:831–837.
4. Reeps C, Essler M, Pelisek J, Seidl S, Eckstein HH, Krause BJ. Increased ^{18}F-fluorodeoxyglucose uptake in abdominal aortic aneurysms in positron emission/computed tomography is associated with inflammation, aortic wall instability, and acute symptoms. *J Vasc Surg*. 2008;48:417–423.
5. Rudd JH, Myers KS, Bansilal S, et al. ^{18}Fluorodeoxyglucose positron emission tomography imaging of atherosclerotic plaque inflammation is highly reproducible: implications for atherosclerosis therapy trials. *J Am Coll Cardiol*. 2007;50:892–896.
6. Ogawa M, Magata Y, Kato T, et al. Application of ^{18}F-FDG PET for monitoring the therapeutic effect of antiinflammatory drugs on stabilization of vulnerable atherosclerotic plaques. *J Nucl Med*. 2006;47:1845–1850.
7. Tahara N, Kai H, Ishibashi M, et al. Simvastatin attenuates plaque inflammation: evaluation by fluorodeoxyglucose positron emission tomography. *J Am Coll Cardiol*. 2006;48:1825–1831.
8. Rudd JH, Myers KS, Bansilal S, et al. Atherosclerosis inflammation imaging with ^{18}F-FDG PET: carotid, iliac, and femoral uptake reproducibility, quantification methods, and recommendations. *J Nucl Med*. 2008;49:871–878.
9. Lee SJ, On YK, Lee EJ, Choi JY, Kim BT, Lee KH. Reversal of vascular ^{18}F-FDG uptake with plasma high-density lipoprotein elevation by atherogenic risk reduction. *J Nucl Med*. 2008;49:1277–1282.
10. von Schulthess GK, Steinert HC, Hany TF. Integrated PET/CT: current applications and future directions. *Radiology*. 2006;238:405–422.
11. Shimizu K, Mitchel RN, Libby P. Inflammation and cellular immune responses in abdominal aortic aneurysms. *Arterioscler Thromb Vasc Biol*. 2006;26:987–994.
12. Wu YW, Kao HL, Chen MF, et al. Characterization of plaques using ^{18}F-FDG PET/CT in patients with carotid atherosclerosis and correlation with matrix metalloproteinase-1. *J Nucl Med*. 2007;48:227–233.
13. Tahara N, Kai H, Nakaura H, et al. The prevalence of inflammation in carotid atherosclerosis: analysis with fluorodeoxyglucose-positron emission tomography. *Eur Heart J*. 2007;28:2243–2248.
14. Sakalihasan N, Van Damme H, Gomez P, et al. Positron emission tomography (PET) evaluation of abdominal aortic aneurysm (AAA). *Eur J Vasc Endovasc Surg*. 2002;23:431–436.
15. Davies JR, Rudd JH, Fryer TD, et al. Identification of culprit lesions after transient ischemic attack by combined ^{18}F fluorodeoxyglucose positron-emission tomography and high-resolution magnetic resonance imaging. *Stroke*. 2005;36:2642–2647.
16. Okane K, Ibaraki M, Toyoshima H, et al. ^{18}F-FDG accumulation in atherosclerosis: use of CT and MR co-registration of thoracic and carotid arteries. *Eur J Nucl Med Mol Imaging*. 2006;33:589–594.
17. Arauz A, Hoyos L, Zenteno M, Mendoza R, Alexanderson E. Carotid plaque inflammation detected by ^{18}F-fluorodeoxyglucose-positron emission tomography: pilot study. *Clin Neurol Neurosurg*. 2007;109:409–412.
18. Tahara N, Kai H, Yamagishi S, et al. Vascular inflammation evaluated by [^{18}F]-fluorodeoxyglucose positron emission tomography is associated with the metabolic syndrome. *J Am Coll Cardiol*. 2007;49:1533–1539.
19. Kuehl H, Eggebrecht H, Boes T, et al. Detection of inflammation in patients with acute aortic syndrome: comparison of FDG-PET/CT imaging and serologic markers of inflammation. *Heart*. 2008;94:1472–1477.
20. Paulmier B, Duet M, Khayat R, et al. Arterial wall uptake of fluorodeoxyglucose on PET imaging in stable cancer disease patients indicates higher risk for cardiovascular events. *J Nucl Cardiol*. 2008;15:209–217.

The Journal of NUCLEAR MEDICINE

Vascular Inflammation Imaging with ^{18}F-FDG PET/CT: When to Image?

Leon J. Menezes, Carl W. Kotze, Brian F. Hutton, Raymondo Endozo, John C. Dickson, Ian Cullum, Syed W. Yusuf, Peter J. Ell and Ashley M. Groves

This article and updated information are available at:
http://jnm.snmjournals.org/content/50/6/854

Information about reproducing figures, tables, or other portions of this article can be found online at:
http://jnm.snmjournals.org/site/misc/permission.xhtml

Information about subscriptions to JNM can be found at:
http://jnm.snmjournals.org/site/subscriptions/online.xhtml

SOCIETY OF
NUCLEAR MEDICINE
AND MOLECULAR IMAGING